Carbohydrate Polymers 183 (2018) 192–200

Contents lists available at ScienceDirect

Carbohydrate Polymers

journal homepage: www.elsevier.com/locate/carbpol

2,3-Di-*O*-sulfo glucuronic acid: An unmodified and unusual residue in a highly sulfated chondroitin sulfate from *Litopenaeus vannamei*

Rômulo S. Cavalcante[a,b,1], Adriana S. Brito[a,c,1], Lais C.G.F. Palhares[a], Marcelo A. Lima[d,e], Renan P. Cavalheiro[d], Helena B. Nader[d], Guilherme L. Sassaki[f,*], Suely F. Chavante[a,**]

[a] Programa de Pós-graduação em Bioquímica e Biologia Molecular, Departamento de Bioquímica, Universidade Federal do Rio Grande do Norte, Natal, RN, Brazil
[b] Programa de Pós-graduação em Ciências da Saúde, Departamento de Morfologia, Universidade Federal do Rio Grande do Norte, Natal, RN, Brazil
[c] Faculdade de Ciências da Saúde do Trairi, Universidade Federal do Rio Grande do Norte, Santa Cruz, RN, Brazil
[d] Departamento de Bioquímica, Universidade Federal de São Paulo, SP, Brazil
[e] Department of Biochemistry, University of Liverpool, Liverpool, L69 7ZB, United Kingdom
[f] Departamento de Bioquímica e Biologia Molecular, Universidade Federal do Paraná, Curitiba, PR, Brazil

ARTICLE INFO

Keywords:
Chondroitin sulfate
NMR spectroscopy
Structural caracterization
Litopenaeus vannamei

ABSTRACT

The occurrence of a natural and unmodified highly sulfated chondroitin sulfate from *Litopenaeus vannamei* heads (sCS) is herein reported. Its partial digestion by Chondroitinases AC and ABC together with its electrophoretic migration profile revealed it as a highly sulfated chondroitin sulfate despite its average molecular weight being similar to CSA. Using orthogonal 1D/2D NMR experiments, the anomeric signals (δ 4.62/106.0) corresponding to unusual 2,3-di-*O*-Sulfo-GlcA (~36%), $U3_{3S}$ (δ 4.42/84.1, ~63%) and $U2_{2S}$ (4.12/80.1, ~50%) substitutions were confirmed. In addition, non-sulfated GlcA (δ 4.5/106.3) linked to 4-*O*- ($A1_{4S}$, 36%) or 6-*O*-Sulfo ($A1_{6S}$, 28%) GalNAc (δ 4.64/103.5) was observed. Although the biological role of sCS in shrimp is unknown, its influence on hemostasis was also demonstrated. The sCS identification brings to light new questions about the hierarchical model of GAGs biosynthesis and contributes to the better understanding of the subtle relationship between GAGs structure and function.

1. Introduction

Chondroitin sulfate (CS) is a sulfated polysaccharide, part of a class of natural and highly complex biomolecules known as glycosaminoglycans (GAGs). These molecules are widely distributed throughout the cell surface and all extracellular matrix of connective tissues and are covalently attached to a protein core forming proteoglycans (CSPGs) (Schiller et al., 2015; Wang, Sugahara, & Li, 2016). CS is composed by repeating disaccharide units which occur along the polysaccharide chain linked by $\beta(1 \rightarrow 4)$ bonds, where each disaccharide is formed by *D*-glucuronic acid (GlcA) $\beta(1 \rightarrow 3)$ linked to N-acetyl-*D*-galactosamine (GalNAc) (Lamari & Karamanos, 2006; Prabhakar & Sasisekharan, 2006; Tomatsu et al., 2015). The variations of the *O*-sulfation pattern observed for both GalNAc and GlcA generate different combinations of distinct disaccharide units that characterize the several types of CS. GalNAc residues are often sulfated at the C-4 and/or C-6 positions which can give rise to CS-A [GlcA-GalNAc(4S)], CS-C [GlcA-GalNAc (6S)] and CS-E [GlcA–GalNAc(4S,6S)] units. On the other hand, GlcA residues may exhibit O-sulfation at C-2 and more rarely at C-3 positions giving rise to CS-D [GlcA(2S)-GalNAc(6S)] and CS-K [GlcA(3S)-GalNAc (4S)] units, respectively (Malavaki, Mizumoto, Karamanos, & Sugahara, 2008; Nandini & Sugahara, 2006; Pavão, Vilela-Silva, & Mourão, 2006).

The position and degree of sulfation, size and number of CS chains inserted into the CSPGs, make CS a highly complex and heterogeneous molecule that exert multifaceted functions (Mikami & Kitagawa, 2013; Volpi, 2011). Among the many functions attributed to CS chains, there are some important biological processes such as inflammation, cell proliferation, differentiation, migration, tissue morphogenesis, organogenesis, infections and wound repair (Canning, Brelsford, & Lovett, 2016; Sugahara et al., 2003; Tomatsu et al., 2015; Yamada & Sugahara, 2008). In addition, a significant chemical and structural diversity of CS chains can also be observed according to the animal tissue- and species-source. Consequently, these structural variations lead to different biological and pharmacological properties (Maccari, Ferrarini, & Volpi, 2010; Malavaki et al., 2008). Evidence shows that in invertebrates species such structural heterogeneity is even more pronounced

* Corresponding author at: Department of Biochemistry and Molecular Biology, Federal University of Paraná, Curitiba, PR, Brazil.
** Corresponding author at: Biochemistry Department, Federal University of Rio Grande do Norte, Natal, RN, Brazil.
E-mail addresses: guilherme.sassaki@gmail.com (G.L. Sassaki), chavantesu@hotmail.com (S.F. Chavante).
[1] These authors contributed equally to this work.

https://doi.org/10.1016/j.carbpol.2017.12.018
Received 24 May 2017; Received in revised form 7 December 2017; Accepted 9 December 2017
Available online 13 December 2017
0144-8617/

(Malavaki et al., 2008), as in the case of the Echinodermata sea cucumber, which has a CS *O*-substituted at C-3 position on GlcA residues with sulfated α-*L*-fucopyranosyl branches. Such fucosylated CS presented different biological functions when compared to its defucosylated counterpart, as anticoagulant and antithrombotic activities (Fonseca & Mourão, 2006; Wu et al., 2015).

Within this context and given the great structural and functional complexity of CS molecules from different species, here we report the occurrence of a natural and structurally peculiar CS. This compound was isolated from the cephalothorax (head) of Pacific white shrimp, *Litopenaeus vannamei*, the major farmed shrimp specie in the Northeast of Brazil and in the world (Cahú et al., 2012).

2. Experimental

2.1. General experimental procedures

Sodium heparin from porcine mucosa was obtained from Laboratory Derivati Organici (Trino Vercellese, Italy). Synthetic heparin pentasaccharide was obtained from GSK (Rio de Janeiro, Brazil). Chondroitinase ABC from *Proteus vulgaris* (EC 4.2.2.4), specific activity of 50–250 units/mg, and chondroitinase AC from *Flavobacterium heparinum* (EC 4.2.2.5), specific activity of 0.5–1.5 units/mg; 1,3-diaminopropane (PDA); bovine serum albumin (BSA) and heparin cofactor II from Sigma-Aldrich Co. (St. Louis, USA). Agarose low-Mr from Bio-rad (Richmond, USA). Chondroitin 4-sulfate (CS-4) and chondroitin 6-sulfate (CS-6), extracted from whale cartilage, and dermatan sulfate (DS) extracted from pig skin, were from Miles Laboratories (Elhart, USA). aPTT and PT kits were obtained from Wiener Lab. (Rosario, Argentina). Anti-Xa and anti-IIa kits and chromogenic substrates for thrombin (*D*-Phe-Pip-Arg-pNa) were purchased from Hyphen BioMed (Neuville-sur-Oise, France). Carrier free [^{35}S]-inorganic sulfate was purchased from Instituto de Pesquisas Nucleares (São Paulo, Brazil).

2.2. Cell cultures

Endothelial cells derived from rabbit aorta were grown in F12 medium (Invitrogen, San Diego, USA) containing 10% fetal bovine serum (FBS) (Cultilab, Campinas, Brazil) and 20 mM sodium bicarbonate at 37 °C in a humidified atmosphere with 5% CO_2. All cultures were performed on Falcon culture plates (BD Falcon, San Jose, USA).

2.3. Animals

Male Wistar rats weighing between 300 and 400 g, obtained from the animal house of Departamento de Bioquímica – Universidade Federal do Rio Grande do Norte, Natal, Brazil, were used for *in vivo* experiments. Animals were housed in cages with free access to food and water. Animals were treated according to the ethical principles for animal experimentation. All experiments were approved by the university Ethics Committee (number 053/2011).

The shrimp heads (*Litopenaeus vannamei*) were kindly provided by ENSEG Indústria Alimentícia LTDA, Macaíba, Brazil. The fresh material was stored on ice until processing.

2.4. Extraction and purification of the sCS

The GAGs were isolated and purified from *L. vannamei* heads (~14 kg) after proteolysis and acetone fractionation as previously described (Brito et al., 2008, 2014) with some modifications. Briefly, the fractions obtained after treatment with acetone (F-0.5, F-0.7 and F-1.0) were individually submitted to ion-exchange chromatography in Dowex 50W-X8 Na + -form (Aldrich). F-0.7 was further fractioned by ion-exchange chromatography in DEAE-Sephacel (Pharmacia) and desalted using Sephadex G-25 gel filtration. The final product was dried and submitted to further analysis.

2.5. Electrophoresis

GAGs identification was done by agarose gel electrophoresis using 0.05 M 1,3-diaminopropane acetate (PDA) buffer system, pH 9.0 (Dietrich & Dietrich, 1976) or discontinuous buffer 0.04 M barium acetate, pH 5.8/0.05 M 1,3-diaminopropane acetate, pH 9.0 (Ba/PDA) (Bianchini et al., 1980). Aliquots of the compounds (5–10 μL) were applied to a 0.5% agarose gel and ran for 1 h at 100 V. The GAGs were fixed with 0.1% cetyltrimethylammonium bromide solution. After 2 h, the gels were dried and stained for 15 min with 0.1% toluidine blue in 1% acetic acid in 50% ethanol. The gels were then destained with the same solution without the dye.

2.6. Molecular weight determination

The molecular weight (MW) of sCS was determined by gel permeation chromatography on a high-pressure liquid chromatography (GPC-HPLC) system using a 300 × 7.8 mm BioSep SECTM S-2000 LC Column (Phenomenex, Torrance, USA). 20 μL aliquots of a sample solution (10 mg/mL in 0.3 M sodium sulfate) were applied into the GPC-HPLC system at a flow rate of 1 mL/min. UV detection was performed at 205 nm at room temperature. The column was previously calibrated with polysaccharides of known molecular weights (1.7, 4, 10, 16, 20, 26 and 67 KDa).

2.7. Structural characterization

For NMR experiments, the purified sCS were deuterium exchanged by repeated dissolution in D_2O and freeze-drying. Spectra were obtained in D_2O in a shigemmi (200 μL) tube at 30 °C or 70 °C, using TMSPd_4 as standard (δ = 0). 2D-MNR [COSY, TOCSY (mixing time, 100 ms) and NOESY (mixing time, 400 ms)] spectra were obtained with a Bruker 600 MHz AVANCE III NMR spectrometer with a 5 mm inverse gradient probe (QXI). HSQC and HSQC-TOCSY (mixing time, 60 ms) with spectral widths of 7211 Hz (1H) and 12,073 Hz (^{13}C) were recorded for quadrature detection in the indirect dimension, using 64 or 128 scans per series of 2 K x 256 and a width data points with zero filling in F1 (2 K) prior to Fourier transformation (Sassaki et al., 2013). All signal assignments were performed using TopSpin program. 1D TOCSY experiments were carried out using a standard Bruker pulse program (selmlgp). A shaped pulse length of 80 ms for selective excitation was used, followed by a MLEV-17. Selective pulses of different mixing times varying from 5 to 100 ms using 256 scans were used.

Disaccharide composition of the sCS was assessed as described by Yamagata, Saito, Habuchi, and Suzuki (1968) with some modification. Purified sCS (~100 μg) was incubated with 25 mIU of chondroitinase AC or ABC. The products obtained were analyzed by agarose gel in PDA buffer and HPLC in a 150 × 4.6 mm Phenosphere SAX column (Phenomenex, Torrance, USA) using a NaCl gradient of 0.01–2 M with at a flow of 1 ml/min and UV detection at 232 nm.

2.8. In vitro anticoagulants assays

Anticoagulant activity of the sCS was evaluated by different assays according to the kits manufacturer's recommendation. The activated partial thromboplastin time and prothrombin time were measured using the Quick Timer Coagulometer (Drake Electronica Commerce Ltd., São Paulo, Brazil). Initially, 90 μL of fresh human citrated plasma was incubated with 10 μL of mammalian heparin or purified sCS at different concentrations or saline as control. After 3 min of incubation at 37 °C, cephalin and later calcium chloride (for APTT) or a mixture of thromboplastin, calcium chloride and sodium chloride (for PT), were then added and the clotting time assessed. All assays were performed in triplicate.

2.9. Chromogenic assays

The sCS had also its anti-Xa and anti-IIa activities assessed through the chromogenic assays. Briefly, antithrombin (for anti-Xa assay) or thrombin (for anti-IIa assay) was incubated with mammalian heparin or purified sCS in different concentrations at 37 °C for 2 min. After incubation, purified bovine Xa or IIa factors was added, mixed and incubated at 37 °C for 2 min. Next, the chromogenic substrate for Xa or IIa factors was added and the mixture incubated again for 2 min at 37 °C. Then, to stop the reaction, 30% acetic acid was added and absorbance measured at 405 nm against a corresponding blank using a microplate reader (BioTek Epoch, Winooski, USA). The inhibition of thrombin by heparin cofactor II was carried out as follows: using 96-well microplates, mammalian heparin or purified sCS (0–100 μg/ml) was incubated with 70 nM heparin cofactor II and 15 nM thrombin (Seikisui Diagnostics, Stamford, USA) in 25 μl of 0.02 M Tris/HCl, 0.15M NaCl, and 1.0 mg/ml polyethylene glycol, pH 7.4 (TS/PEG buffer). Thrombin was added last to initiate the reaction. After 60 s of incubation at room temperature, 25 μL of 100 μM thrombin chromogenic substrate in TS/PEG buffer was added, and the absorbance at 405 nm was recorded at 10 s intervals for 100 s. The rate of change of absorbance was proportional to the thrombin activity remaining in the incubation and the results were expressed by percentage of thrombin inhibition. All assays were performed in triplicate.

2.10. Differential scanning fluorimetry (DSF)

DSF experiments were performed using a 7500 Real Time PCR System (Applied Biosystems, Warrington, U.K.) as described previously (Uniewicz et al., 2010). Briefly, antithrombin solution (1 mg/mL), mammalian heparin, sCS solution (1 mg/mL) or PBS without $CaCl_2$/$MgCl_2$ (Gibco-Europe, Paisley, U.K.) (70% v/v) were added to a Fast Optical 96 Well Reaction Plate (Applied Biosystems) maintained on ice. Then, freshly prepared 100 x water based dilution of Sypro Orange 5000 x (Invitrogen, Paisley, U.K.) was added as 10% v/v. The dye has an excitation wavelength of 300 or 470 nm, and emits at 570 nm when bound to hydrophobic residues. The protein was subjected to a stepwise temperature gradient, from 32 °C to 85 °C in 0.5 °C steps. There was an initial 2 min incubation period at 31 °C and 5 s between each temperature increase to equilibrate. Data were collected for 30 s at each temperature.

2.11. Antithrombotic activity in vivo

Rats had the inferior vena cava exposed and a ligature was performed with cotton thread, 5 min after intravenous injection of mammalian heparin or sCS in 0.2 mL of saline. The abdominal cavity was then closed. After 2 h, the vein was exposed again and the eventual thrombi formed were removed, washed, blotted with filter paper, dried under vacuum for 24 h and weighed. At each dose, six measurements were performed (Reyers, Mussoni, Donati, & de Gaetano, 1980; Rocha et al., 2005).

2.12. Effect of sCS on glycosaminoglycans synthesis by endothelial cells

Endothelial cells was exposed to mammalian heparin or sCS and carrier free [^{35}S]-sulfate (150 μCi/mL) at 37 °C in a humidified incubator at 5% CO_2. After 24 h of incubation, the culture medium was removed and the cells washed twice with serum-free F12 medium. Protein-free heparan sulfate and chondroitin sulfate chains were obtained from the cell extract and culture medium by incubating the sample with 0.1 mg of superase (proteolytic enzyme from *Sporobacillus*, Chas & Pfizer, USA) for 4 h at 60 °C. At the end of the incubation, the mixture was heated for 7 min at 100 °C to inactivate the protease, and the radiolabeled glycosaminoglycans were precipitated with two volumes of methanol in the presence of carrier heparan sulfate and chondroitin sulfate (5 μg/μL). The heparan sulfate and chondroitin sulfate synthesized by these cells and secreted to the medium were quantified and characterized by their electrophoretic mobility in agarose gel. The radiolabelled compounds were visualized by exposure of the gel after drying and staining to a Kodak blue X-rayfilm. The radioactive bands were scrapped from the gel and counted in a liquid scintillation counter using Ultima Gold (Packard Instruments Co, Groningen, Holland). All experiments were performed in triplicate.

2.13. Bleeding effect

The residual hemorrhagic effect of sCS was analyzed by a modified model of topical scarification in rat tail (Cruz & Dietrich, 1967). A scarification was made with a surgical blade in the tail distal portion of rats. Next, the scarified tail was dipped vertically in physiological saline solution, and the blood flow was stimulated with a scraped and dipped again in fresh saline to observe bleeding. Then, the tail was dipped in a solution containing sCS or heparin at different concentrations during 2 min and washed extensively with saline solution. The treated tail was immersed in new saline solutions during 40 min, and the amount of protein from the lesion was determined by Bradford method (Bradford, 1976). The results were expressed as the sum of the protein values of each tube minus the amount of protein present before the exposure to the test substance.

2.14. Statistical analysis

Results were analyzed by two-way ANOVA and Bonferroni posttest. Values of $p < 0.05$ were considered indicative of statistical significance.

3. Results and discussion

3.1. Identification and structural characterization of sCS

The GAGs isolated from *L. vannamei* shrimp heads (~960 mg) were treated with increasing volumes of acetone and the resulting fraction of treatment with 0.7 volumes of acetone (F-0.7, ~233 mg) was subjected to ion exchange chromatography on DEAE-Sephacel, from which the shrimp CS-like compound (sCS) was purified (~105 mg, Fig. S1, Supporting information). Its molecular weight was determined by GPC and it was estimated as 26 kDa, the same average molecular weight found for bovine tracheal CS (Lamari & Karamanos, 2006).

The structural characterization of sCS was achieved using homonuclear (selective 1D-TOCSY, COSY, TOCSY and NOESY) and heteronuclear (HSQC and HSQC-TOCSY) NMR spectroscopy. Following these procedures, it was possible to assign the hydrogen and carbon resonances and a chemical shift map of $^{1}H/^{13}C$ atoms (2D $^{1}H/^{13}C$ HSQC), shown in the Fig. 1. As noted in the HSQC spectrum, the anomeric signals identified at δ 4.62/106.0, which corresponds to 2-*O*- ($U1_{2S}$) and 3-*O*-Sulfo GlcA ($U1_{3S}$) and non-sulfated GlcA at δ 4.5/106.3, U1 linked to 4-*O*- ($A1_{4S}$) or 6-*O*-Sulfo ($A1_{6S}$) GalNAc residues at δ 4.64/103.5 (Gargiulo, Lanzetta, Parrilli, & De Castro, 2009; Gomes et al., 2010; Kinoshita-Toyoda et al., 2004; Mucci, Schenetti, & Volpi, 2000). No signals corresponding to iduronic acid (IdoA) were found, which characterizes the occurrence of typical CS molecule backbone in the shrimp heads.

In order to further characterize the sCS structure and confirm the 2,3-di-*O*-Sulfo GlcA units, selective 1D-TOCSY experiments were performed with different mixing times (Fig. 1, green and red spectrum). From the overlap of the 1D-TOCSY and 2D $^{1}H/^{13}C$ HSQC spectra, the 3-*O*-sulfation *J*-coupling within the GlcA spin system was observed. The chemical shift at δ 4.42/84.1 corresponding to $U3_{3S}$ was the selected spin for magnetic excitation, then the spectra were collected with 20 ms (green spectrum) and 100 ms (red spectrum) mixing times. With short mixing time (20 ms) the protons signals represented by *b* and *c* peaks

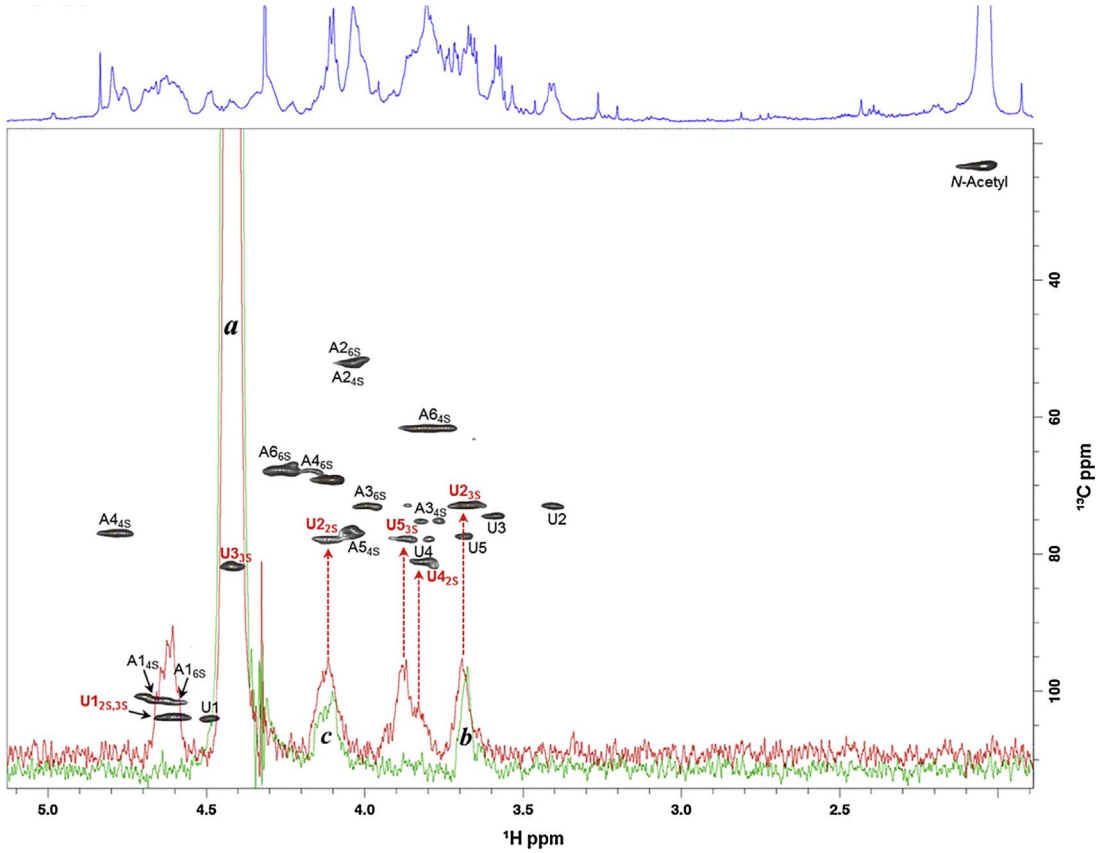

Fig. 1. $^{1}H/^{13}C$ HSQC and 1D TOCSY RMN spectra of sCS. Spectra were obtained at 600 MHz from solutions in D_2O at 30 °C, using TMSPd_4 as standard. 1D TOCSY spectra were collected at 20 ms (green spectrum) and 100 ms (red spectrum) mixing times. Proton signal selected to magnetic excitation (a) and closest correlated signals (b and c); Galactosamine (A); Glucuronic acid (U). (For interpretation of the references to color in this figure legend, the reader is referred to the web version of this article.)

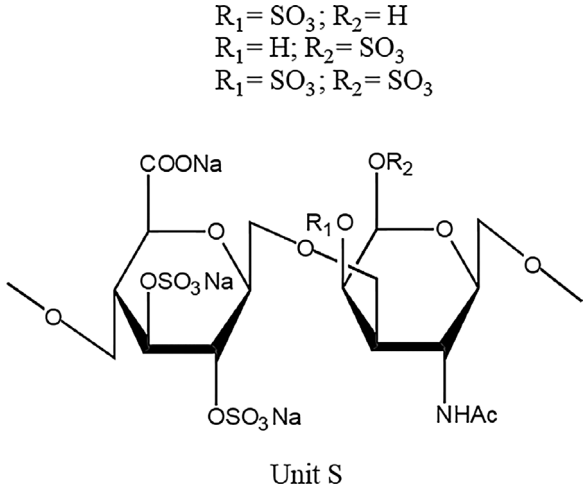

Fig. 2. Proposed structure for the peculiar disaccharide unit found in sCS.

were observed as the closest to the selected peak (*a*), respectively, due the vicinal scalar coupling. Owing to this fact, it is possible to confirm the 2,3-di-*O*-Sulfo GlcA residues occurrence in the sCS chains, besides the 2-*O*-, 3-*O*-Sulfo and non *O*-Sulfo GlcA residues as previously mentioned.

2D COSY experiments were employed to corroborate such results and identify vicinal couplings, mainly H1-H2 and H2-H3/H4 resonances belonging to the non *O*-Sulfo glucuronyl units. The same approach led to the identification of the hydrogen units from 4/6-*O*-GalNAc and the unusual *O*-sulfation in the glucuronyl units of sCS (Figs. S2–S4, Supporting information).

2D TOCSY analyses with mixing time of 100 ms confirmed the connectivity of the monosaccharides from the sCS and supported the previous assignments from COSY cross peaks (Fig. S5, Supporting information). In order to complete the hydrogen assignment by homonuclear experiments, 2D heteronuclear HSQC and HSQC-TOCSY were used to resolve some peak superimposition (Fig. S6, Supporting information). The data set obtained enabled the chemical shift assignments of sCS and are shown in table S1 (Supporting information).

The natural occurrence of 2,3-di-*O*-Sulfo GlcA residues in CS chains is unusual and hitherto unknown [although has been related to products derived from semi-synthetic routes and/or those associated with the heparin contamination crisis (Bedini et al., 2012; Guerrini et al., 2008; Li et al., 2009; Zhang et al., 2008)], and the description of such sulfation pattern in sCS chains may explain its resistance to chondroitinases action (Linhardt, 2001; Maruyama, Toida, Imanari, Yu, & Linhardt, 1998). As result, unsaturated disaccharide formation was not observed even after exhaustive treatment of sCS with specific lyases (data not shown).

It is important to note that 3-*O*-Sulfo GlcA residues was observed in the linkage region of CS chains and also in some glycoproteins and glycolipids saccharide sequence in mammals (Ariga et al., 1987; Ilyas, Dalakas, Brady, & Quarles, 1986; Nakagawa, Izumikawa, Kitagawa, & Oka, 2011; Voshol, van Zuylen, Orberger, Vliegenthart, & Schachner, 1996). In both cases it has been shown that 3-*O*-sulfation reactions share the same 3-*O*-sulfotransferase (Hashiguchi et al., 2011; Nakagawa et al., 2011). On the other hand, although 3-*O*-Sulfo GlcA residues have been identified in CS chains of marine invertebrate sources (Kinoshita et al., 1997, 2001; Kinoshita-Toyoda et al., 2004; Kitagawa et al., 1997; Sugahara et al., 1996), no 3-*O*-sulfotransferase responsible for such process has been characterized, and its biosynthetic mechanisms cannot be encapsulated within the hierarchical model for GAG biosynthesis.

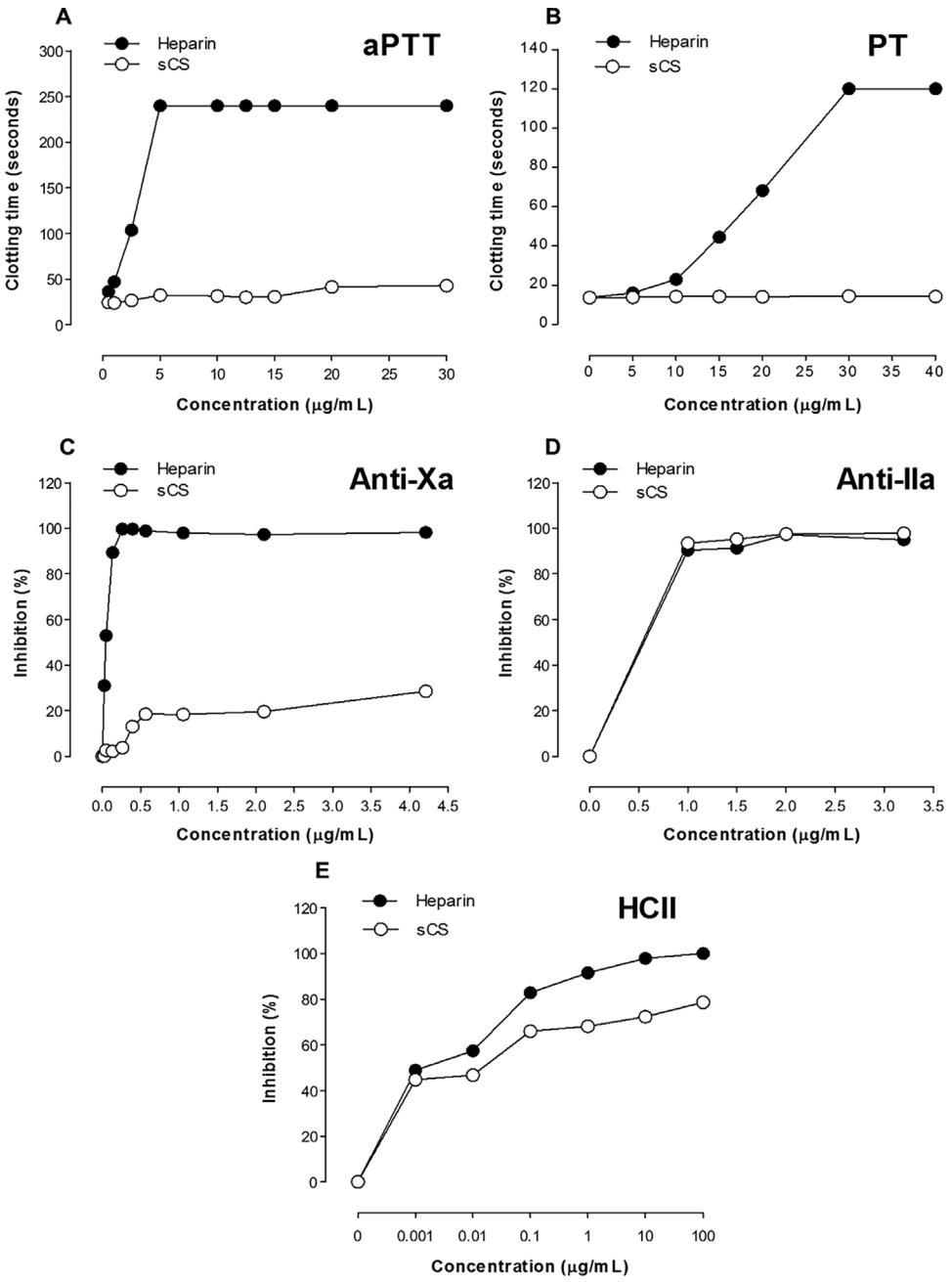

Fig. 3. Anticoagulant assays of sCS. aPTT (A) and PT (B) were performed using citrated normal human plasma, and the clotting time measured in coagulometer. Anti-Xa (C), anti-IIa (D) and HCII (E) activities were performed using specific chromogenic substrates as described in methods. All assays were performed in triplicate and the values are expressed as the mean. sCS (white circle) and heparin (black circle).

The lack of information regarding the identification of unusual 2,3-di-*O*-Sulfo GlcA residue in CS chains from animal tissues, led us to propose a novel disaccharide unit classification for this molecule. Full interpretation of HSQC spectrum also provides the possibility to integrate the cross peak volumes of selected glycosyl units. The later gave rise to 36% of 2,3-di-*O*-Sulfo GlcA residues in sCS, being observed at δ 4.62/103.0. The sulfation pattern from the galactosamine units showed $A1_{4S}$ at δ 4.65/103.0 (36%) and $A1_{6S}$ at δ 4.62/103.5 (28%). The total sulfation of $U3_{3S}$ (δ 4.42/84.1) and $U2_{2S}$ (δ 4.12/80.1) had a percentage of 63% and 50%, respectively. Therefore, in recognition of its obtaining source (Shrimp), the unit S classification is proposed to all disaccharide from CS containing the unusual GlcA residue, regardless of their adjacent galactosamine (Fig. 2). Thus, CS chains where the unit S is found may be recognized as CS-S.

3.2. Anticlotting activities and sCS effect on antithrombin thermal stabilization

As previously noted, the structural variations observed in CS chains from different tissues/species – especially in marine organisms – may result in very different biological and/or pharmacological effects (Maccari et al., 2010; Malavaki et al., 2008). It has been reported, for example, that the sulfation pattern plays an important role in the anticoagulant activity of CS (Maruyama et al., 1998). Thus, the occurrence of highly sulfated units in sCS led us to investigate its effect on coagulation.

The anticoagulant activity of sCS was performed by different assays and compared to porcine heparin action – standard anticoagulant drug. Briefly, activated partial thromboplastin time (aPTT) and prothrombin time (PT) evaluate the components involved in the intrinsic and extrinsic coagulation cascade pathway, respectively. As seen in Fig. 3A and B, unlike porcine heparin, sCS was unable to change the clotting

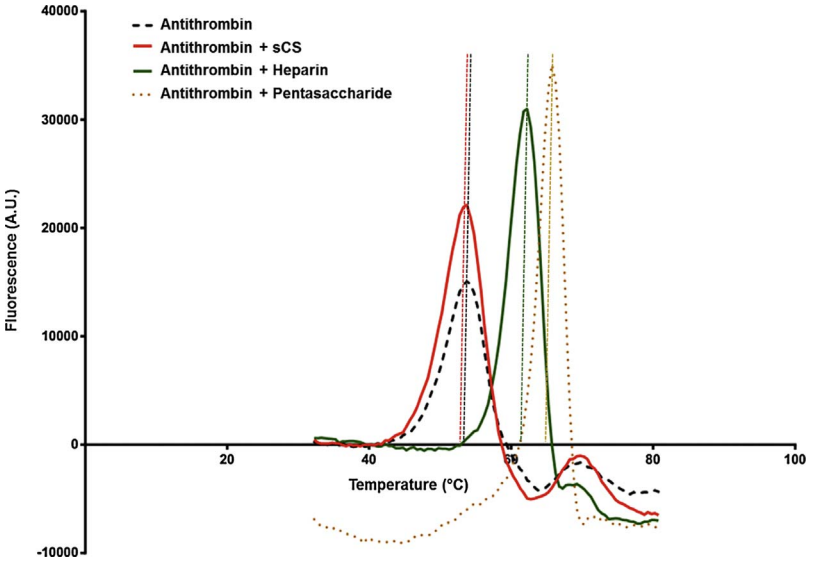

Fig. 4. Effect of sCS on thermo-stabilization of antithrombin evaluated by differential scanning fluorimetry. Melting curve profile of 30 nM antithrombin in the presence or absence of different ligands. Dotted vertical lines indicate the average melting temperature of antithrombin. Antithrombin (black dashed line); antithrombin + sCS (red solid line); antithrombin + heparin (green solid line); antithrombin + pentasaccharide (brown dotted line). (For interpretation of the references to color in this figure legend, the reader is referred to the web version of this article.)

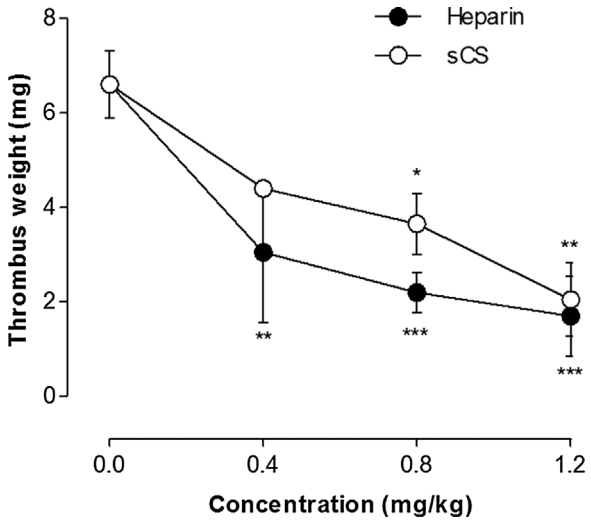

Fig. 5. *In vivo* antithrombotic effect of sCS (white circle) and heparin (black circle) estimated by venous thrombosis-induced model in rats. The asterisks represent statistically significant points ($P < 0.01$*; $P < 0.01$** and $P < 0.001$***) compared to control (0 mg/kg) according to ANOVA (two-way) test and Bonferroni post-test. The bars indicate the standard error of the measurements.

time. A specific analysis for factor Xa (FXa) and thrombin (FIIa) inhibition were performed using chromogenic assays (Fig. 3C and D) and showed that sCS has no effect on factor Xa inhibition (28% of inhibition versus 98% for heparin). On the other hand, both heparin and sCS showed a significant FIIa inhibition of ~94%, even at low concentration (1.0 μg/mL).

In order to investigate the mechanisms by which sCS is able to promote the FII inhibition, experiments involving differential scanning fluorimetry (DSF) and heparin cofactor II (HCII) assay were carried out. As seen in Fig. 4, when compared to heparin or pentasaccharide (heparin saccharide sequence responsible for binding to antithrombin – AT), the compound isolated from shrimp do not alters the AT melting temperature, indicating that sCS is unable to promote the AT stabilization. It was previously reported that there is a close relationship between AT thermal stabilization and anticoagulant activity of polysaccharides (Lima et al., 2013). Thus, the inability to stabilize AT explains the lack of anti-Xa effect and anticoagulant activity via aPTT and PT by sCS. On the other hand, as seen in the Fig. 3E, sCS reached ~80% of thrombin inhibition HCII-mediated, explaining, therefore, its potent anti-IIa effect.

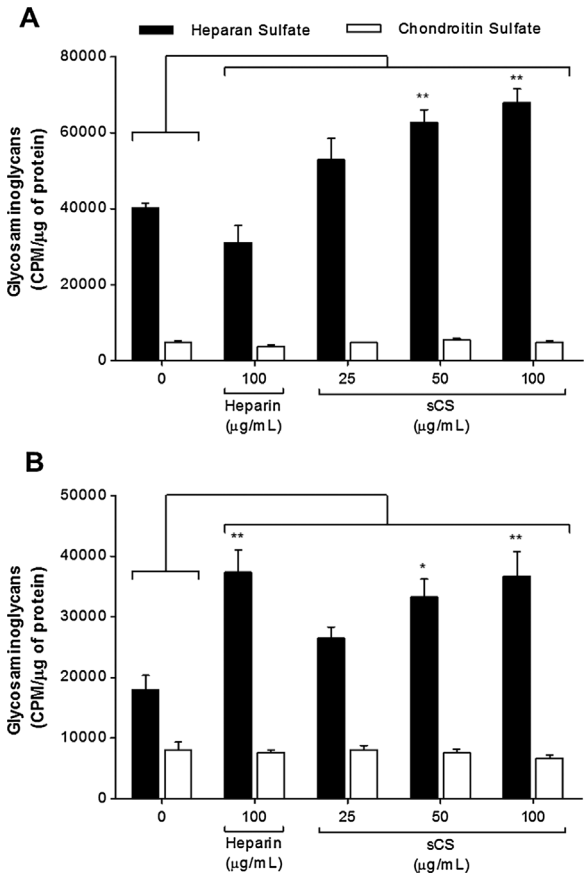

Fig. 6. Effect of sCS and heparin on glycosaminoglycans synthesis by endothelial cells, attached to cell surface (A) and released in the medium (B). Black bars (heparan sulfate); white bars (chondroitin sulfate). The asterisks represent statistically significant points ($P < 0.01$*; and $P < 0.01$**) compared to control (0 μg/kg) according to ANOVA (two-way) test and Bonferroni post-test. The bars indicate the standard error of the measurements.

Some evidences have shown that the anticoagulant activity of GAGs may be affected not only by saccharide sequence of AT binding site or sulfation pattern. Instead, a combination of different factors has played a key role in anticoagulant activity, such as environmental factors, substitution patterns, glycosylation type, stabilization of carbohydrate-

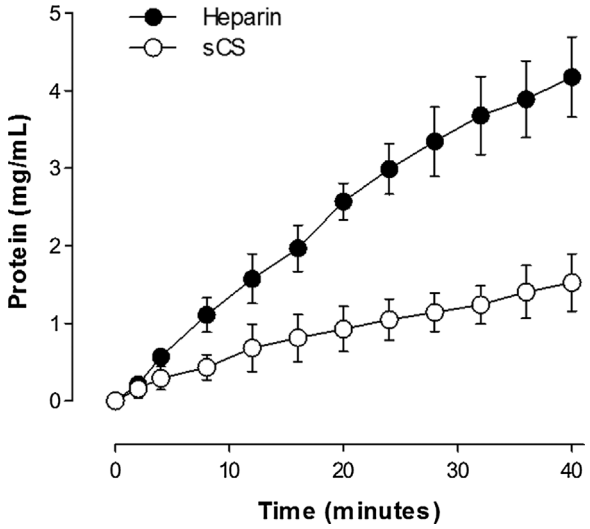

Fig. 7. Hemorrhagic activity in a rat-tail scarification model. 100 µg/mL of sCS (white circle) or heparin (black circle) was applied topically and the bleeding potency measured after 2 min following up to 40 min. The bars indicate the standard error of the measurements.

protein complex, dynamics and conformation (Chavante et al., 2014; Lima et al., 2013; Pomin & Mourao, 2014). In this sense, the conformational changes could also help us to understand the anticoagulant activity of sCS. In their study involving fully *O*-sulfonated chondroitin sulfate, Maruyama et al. showed that 2,3-di-*O*-Sulfo GlcA residues at 30 °C assume the $^1C_4$ conformation, resembling the 2-*O*-sulfo IdoA residue found in heparin. Similarly as occurs with heparin, this conformation strongly favors anti-IIa activity (Maruyama et al., 1998). However, the anti-Xa activity of sCS is remarkably lower than inhibitory capacity of heparin, probably due to inability of sCS to stabilize AT. All these findings corroborate to clarify the complex multifactor relationships that trigger the anticoagulant activity of sCS and others GAGs.

3.3. Antithrombotic activities of sCS

Since FIIa inhibition plays an important role in different hemostasis events, the antithrombotic effect and bleeding potential of sCS were posteriorly analyzed.

The *in vivo* sCS antithrombotic effect was evaluated using an induced venous thrombosis model in rats, as described in methods. The control group only received saline solution and demonstrated 100% of thrombus formation with an average weight of 6.6 ± 0.7 mg (Fig. 5). In contrast, treatment with sCS and heparin resulted in a significant decrease in the thrombus weight and the maximum effect achieved using doses 1.2 mg/kg (~70% of decrease) of both agents.

Based on previous results, the antithrombotic effect *in vivo* observed by sCS may be related to its HCII-mediated anti-IIa activity. Furthermore, the conformational flexibility of 2,3-di-*O*-Sulfo GlcA residues in the sCS chain (Li et al., 2009; Maruyama et al., 1998; Zhang et al., 2008), resembling to IdoA residues, appears to have a relationship with the observed antithrombotic activity (Linhardt et al., 1991). It has also been shown that endothelial cells are target of antithrombotic drugs action, such as heparin and correlated compounds (Boucas et al., 2012; Nader et al., 2001; Nader, Buonassisi, Colburn, & Dietrich, 1989; Nader, Dietrich, Buonassisi, & Colburn, 1987; Rocha et al., 2005; Trindade et al., 2008). When exposed to such compounds, endothelial cells are stimulated to synthesize and release a peculiar heparan sulfate with antithrombotic action. sCS was also able to stimulate the synthesis of such heparan sulfate (Fig. 6A and B) in a dose-dependent manner, in both cellular fraction and secreted to the medium. This, therefore, could be another mechanism by which chondroitin plays antithrombotic effect *in vivo*.

3.4. Hemorrhagic effect

The sCS residual hemorrhagic effect was evaluated after tissue injury induction in rat's tail as described in methods. From the animal model used, when compared to heparin, it was evident that sCS had a lower bleeding potential (Fig. 7). Up to four minutes after contact with the sample, sCS and heparin had the same bleeding potential. Overtime, animals treated with sCS presented less protein content, which represents a lower residual bleeding activity. The high bleeding potential of heparin in the applied methodology is mainly associated to its binding to myosin ATPase molecule in tissue injury region, promoting inhibition of local muscle contractility (Cruz & Dietrich, 1967). Thus, it is possible speculate that sCS is unable to bind to myosin ATPase molecule with the same affinity of mammalian heparin. Other possible mechanism for sCS hemorrhagic effect may be attributed to its higher sulfation degree, which would be responsible to induce the fibrinolytic system through tissue plasminogen activation (Carranza, Durand-Rougley, & Doctor, 2008). Bearing in mind that the animal model used in this study does not favour the contact of sCS with the systemic circulation, the idea that plasminogen may also be activated by sCS locally cannot be discarded.

Although marine invertebrates are devoid of coagulation system similar to those of mammalians, the structural similarities of their GAGs with mammalian heparin (or in this case, oversulfated chondroitin sulfate – OSCS) allows us to observe how GAGs are capable of interacting with proteases from coagulation system and influencing hemostasis events.

A wide range of GAGs with complex and varied saccharidic structures and a very diversified sulfation pattern has been characterized in several marine organisms, including other *L. vannamei* GAGs (Brito et al., 2008, 2014; Chavante et al., 2014). Despite this, the implications that such structural modifications have on the biological role of these marine organisms is not yet fully understood. However, it has been suggested that adverse conditions caused by salinity in the marine environment have influenced the structure of GAGs causing, for example, the increase of the sulfation degree of these molecules. Such modifications would be required to favor interactions with target molecules (Vilela-Silva, Werneck, Valente, Vacquier, & Mourao, 2001).

4. Conclusion

The pharmacological activities attributed to sCS hitherto detached cannot likewise be observed in CS molecules from terrestrial animals. These differences seem to be directly related to the structural peculiarities of sCS, mainly due to the presence of unusual 2,3-di-*O*-Sulfo GlcA residue. Because of similarity between sCS molecules and OSCS found in specific lots of heparin the anticoagulant and antithrombotic effects and the low hemorrhagic potential of sCS should be viewed with caution. However, we must emphasize that the experimental models used in this work as well as the source of sCS molecules are different. Therefore, its ability to exert the same adverse reactions observed for synthetic OSCS cannot be inferred. In another perspective, the information provided here brings to light new questions about the routes capable of explaining how such unusual disulfated residues are synthesized in terms of GAG natural biosynthesis. Furthermore, for both economical and environmental reasons, the identification of a molecule from a low market value sources may provide an attractive waste management in the shrimp farming and carrying out further studies with this GAG.

Supplementary data associated with this article can be found in the online version.

Acknowledgments

This manuscript was support by Grants from CNPq (Conselho Nacional de Desenvolvimento e Tecnológico – Projeto Universal456160/2014-0), CAPES (Coordenação de Aperfeiçoamento de Pessoal de Nível Superior) and FAPESP (Fundação de Amparo a Pesquisa do Estado de São Paulo), Brazil and UFPR NMR Center. Rômulo S. Cavalcante, Laís C.G.F. Palhares and Renan P. Cavalheiro are recipient of fellowships from CAPES.

Appendix A. Supplementary data

Supplementary material related to this article can be found, in the online version, at doi:https://doi.org/10.1016/j.carbpol.2017.12.018

References

Ariga, T., Kohriyama, T., Freddo, L., Latov, N., Saito, M., Kon, K., et al. (1987). Characterization of sulfated glucuronic acid containing glycolipids reacting with IgM M-proteins in patients with neuropathy. *Journal of Biological Chemistry, 262*(2), 848–853.

Bedini, E., De Castro, C., De Rosa, M., Di Nola, A., Restaino, O. F., Schiraldi, C., et al. (2012). Semi-synthesis of unusual chondroitin sulfate polysaccharides containing GlcA(3-O-sulfate) or GlcA(2,3-di-O-sulfate) units. *Chemistry (Weinheim an der Bergstrasse, Germany), 18*(7), 2123–2130.

Bianchini, P., Nader, H. B., Takahashi, H. K., Osima, B., Straus, A. H., & Dietrich, C. P. (1980). Fractionation and identification of heparin and other acidic mucopolysaccharides by a new discontinuous electrophoretic method. *Journal of Chromatography A, 196*(3), 455–462.

Boucas, R. I., Jarrouge-Boucas, T. R., Lima, M. A., Trindade, E. S., Moraes, F. A., Cavalheiro, R. P., et al. (2012). Glycosaminoglycan backbone is not required for the modulation of hemostasis: Effect of different heparin derivatives and non-glycosaminoglycan analogs. *Matrix Biology, 31*(5), 308–316.

Bradford, M. M. (1976). A rapid and sensitive method for the quantitation of microgram quantities of protein utilizing the principle of protein-dye binding. *Analytical Biochemistry, 72*, 248–254.

Brito, A. S., Arimateia, D. S., Souza, L. R., Lima, M. A., Santos, V. O., Medeiros, V. P., et al. (2008). Anti-inflammatory properties of a heparin-like glycosaminoglycan with reduced anti-coagulant activity isolated from a marine shrimp. *Bioorganic & Medicinal Chemistry, 16*(21), 9588–9595.

Brito, A. S., Cavalcante, R. S., Palhares, L. C., Hughes, A. J., Andrade, G. P., Yates, E. A., et al. (2014). A non-hemorrhagic hybrid heparin/heparan sulfate with anticoagulant potential. *Carbohydrate Polymers, 99*, 372–378.

Cahú, T. B., Santos, S. D., Mendes, A., Córdula, C. R., Chavante, S. F., Carvalho, L. B., Jr., et al. (2012). Recovery of protein, chitin, carotenoids and glycosaminoglycans from Pacific white shrimp (Litopenaeus vannamei) processing waste. *Process Biochemistry, 47*(4), 570–577.

Canning, D. R., Brelsford, N. R., & Lovett, N. W. (2016). Chondroitin sulfate effects on neural stem cell differentiation. *In Vitro Cellular & Developmental Biology - Animal, 52*(1), 35–44.

Carranza, Y. E., Durand-Rougley, C., & Doctor, V. (2008). Effect of oversulfation on the chemical and biological properties of chondroitin-4-sulfate. *Blood Coagulation & Fibrinolysis, 19*(6), 483–487.

Chavante, S. F., Brito, A. S., Lima, M., Yates, E., Nader, H., Guerrini, M., et al. (2014). A heparin-like glycosaminoglycan from shrimp containing high levels of 3-O-sulfated D-glucosamine groups in an unusual trisaccharide sequence. *Carbohydrate Research, 390*, 59–66.

Cruz, W. O., & Dietrich, C. P. (1967). Antihemostatic effect of heparin counteracted by adenosine triphosphate. *Proceedings of the Society for Experimental Biology and Medicine, 126*(2), 420–426.

Dietrich, C. P., & Dietrich, S. M. C. (1976). Electrophoretic behaviour of acidic mucopolysaccharides in diamine buffers. *Analytical Biochemistry, 70*(2), 645–647.

Fonseca, R. J. C., & Mourão, P. A. S. (2006). Fucosylated chondroitin sulfate as a new oral antithrombotic agent. *Thrombosis and Haemostasis, 96*(12), 822–829.

Gargiulo, V., Lanzetta, R., Parrilli, M., & De Castro, C. (2009). Structural analysis of chondroitin sulfate from Scyliorhinus canicula: A useful source of this polysaccharide. *Glycobiology, 19*(12), 1485–1491.

Gomes, A. M., Kozlowski, E. O., Pomin, V. H., de Barros, C. M., Zaganeli, J. L., & Pavao, M. S. (2010). Unique extracellular matrix heparan sulfate from the bivalve Nodipecten nodosus (Linnaeus, 1758) safely inhibits arterial thrombosis after photochemically induced endothelial lesion. *Journal of Biological Chemistry, 285*(10), 7312–7323.

Guerrini, M., Beccati, D., Shriver, Z., Naggi, A. M., Bisio, A., Capila, I., et al. (2008). Oversulfated chondroitin sulfate is a major contaminant in heparin associated with adverse clinical events. *Nature Biotechnology, 26*(6), 669–675.

Hashiguchi, T., Mizumoto, S., Nishimura, Y., Tamura, J., Yamada, S., & Sugahara, K. (2011). Involvement of human natural killer-1 (HNK-1) sulfotransferase in the biosynthesis of the GlcUA(3-O-sulfate)-Gal-Gal-Xyl tetrasaccharide found in alpha-thrombomodulin from human urine. *Journal of Biological Chemistry, 286*(38), 33003–33011.

Ilyas, A. A., Dalakas, M. C., Brady, R. O., & Quarles, R. H. (1986). Sulfated glucuronyl glycolipids reacting with anti-myelin-associated glycoprotein monoclonal antibodies including IgM paraproteins in neuropathy: Species distribution and partial characterization of epitopes. *Brain Research, 385*(1), 1–9.

Kinoshita-Toyoda, A., Yamada, S., Haslam, S. M., Khoo, K. H., Sugiura, M., Morris, H. R., et al. (2004). Structural determination of five novel tetrasaccharides containing 3-O-sulfated D-glucuronic acid and two rare oligosaccharides containing a beta-D-glucose branch isolated from squid cartilage chondroitin sulfate E. *Biochemistry, 43*(34), 11063–11074.

Kinoshita, A., Yamada, S., Haslam, S. M., Morris, H. R., Dell, A., & Sugahara, K. (1997). Novel tetrasaccharides isolated from squid cartilage chondroitin sulfate E contain unusual sulfated disaccharide units GlcA(3-O-sulfate)beta1-3GalNAc(6-O-sulfate) or GlcA(3-O-sulfate)beta1-3GalNAc. *Journal of Biological Chemistry, 272*(32), 19656–19665.

Kinoshita, A., Yamada, S., Haslam, S. M., Morris, H. R., Dell, A., & Sugahara, K. (2001). Isolation and structural determination of novel sulfated hexasaccharides from squid cartilage chondroitin sulfate E that exhibits neuroregulatory activities. *Biochemistry, 40*(42), 12654–12665.

Kitagawa, H., Tanaka, Y., Yamada, S., Seno, N., Haslam, S. M., Morris, H. R., et al. (1997). A novel pentasaccharide sequence GlcA(3-sulfate)(beta1-3)GalNAc(4-sulfate)(beta1-4)(Fuc alpha1-3)GlcA(beta1-3)GalNAc(4-sulfate) in the oligosaccharides isolated from king crab cartilage chondroitin sulfate K and its differential susceptibility to chondroitinases and hyaluronidase. *Biochemistry, 36*(13), 3998–4008.

Lamari, F. N., & Karamanos, K. N. (2006). Structure of chondroitin sulfate. In N. Volpi (Ed.). *Chondroitin sulfate: Structure, role and pharmacological activity* (pp. 33–48). London: UK Advances in Pharmacology.

Li, B., Suwan, J., Martin, J. G., Zhang, F., Zhang, Z., Hoppensteadt, D., et al. (2009). Oversulfated chondroitin sulfate interaction with heparin-binding proteins: New insights into adverse reactions from contaminated heparins. *Biochemical Pharmacology, 78*(3), 292–300.

Lima, M. A., Hughes, A. J., Veraldi, N., Rudd, T. R., Hussain, R., Brito, A. S., et al. (2013). Antithrombin stabilisation by sulfated carbohydrates correlates with anticoagulant activity. *Medicinal Chemistry Communication, 4*(5), 870–873.

Linhardt, R. J. (2001). Analysis of glycosaminoglycans with polysaccharide lyases. *Current Protocols in Molecular Biology, 17* 17.13.17-17.13.32.

Linhardt, R. J., Al-Hakim, A., Jian, L., Hoppensteadt, D., Mascellani, G., Bianchini, P., et al. (1991). Structural features of dermatan sulfates and their relationship to anticoagulant and antithrombotic activities. *Biochemical Pharmacology, 42*(8), 1609–1619.

Maccari, F., Ferrarini, F., & Volpi, N. (2010). Structural characterization of chondroitin sulfate from sturgeon bone. *Carbohydrate Research, 345*(11), 1575–1580.

Malavaki, C., Mizumoto, S., Karamanos, N., & Sugahara, K. (2008). Recent advances in the structural study of functional chondroitin sulfate and dermatan sulfate in health and disease. *Connective Tissue Research, 49*(3), 133–139.

Maruyama, T., Toida, T., Imanari, T., Yu, G., & Linhardt, R. J. (1998). Conformational changes and anticoagulant activity of chondroitin sulfate following its O-sulfonation. *Carbohydrate Research, 306*(1–2), 35–43.

Mikami, T., & Kitagawa, H. (2013). Biosynthesis and function of chondroitin sulfate. *Biochimica et Biophysica Acta, 1830*(10), 4719–4733.

Mucci, A., Schenetti, L., & Volpi, N. (2000). 1H and 13C nuclear magnetic resonance identification and characterization of components of chondroitin sulfates of various origin. *Carbohydrate Polymers, 41*(1), 37–45.

Nader, H. B., Buonassisi, V., Colburn, P., & Dietrich, C. P. (1989). Heparin stimulates the synthesis and modifies the sulfation pattern of heparan sulfate proteoglycan from endothelial cells. *Journal of Cellular Physiology, 140*(2), 305–310.

Nader, H. B., Dietrich, C. P., Buonassisi, V., & Colburn, P. (1987). Heparin sequences in the heparan sulfate chains of an endothelial cell proteoglycan. *Proceedings of the National Academy of Sciences, 84*(11), 3565–3569.

Nader, H. B., Pinhal, M. A., Bau, E. C., Castro, R. A., Medeiros, G. F., Chavante, S. F., et al. (2001). Development of new heparin-like compounds and other antithrombotic drugs and their interaction with vascular endothelial cells. *Brazilian Journal of Medical and Biological Research, 34*(6), 699–709.

Nakagawa, N., Izumikawa, T., Kitagawa, H., & Oka, S. (2011). Sulfation of glucuronic acid in the linkage tetrasaccharide by HNK-1 sulfotransferase is an inhibitory signal for the expression of a chondroitin sulfate chain on thrombomodulin. *Biochemical and Biophysical Research Communications, 415*(1), 109–113.

Nandini, C. D., & Sugahara, K. (2006). Role of the sulfation pattern of chondroitin sulfate in its biological activities and in the binding of growth factors. In N. Volpi (Ed.). *Chondroitin sulfate: Structure, role and pharmacological activity* (pp. 253–279). London: UK Advances in Pharmacology.

Pavão, M. S. G., Vilela-Silva, A. C., & Mourão, P. A. S. (2006). Biosynthesis of chondroitin sulfate: From the early, precursor discoveries to nowadays, genetics approaches. In N. Volpi (Ed.). *Chondroitin sulfate: Structure, role and pharmacological activity* (pp. 117–140). London: UK Advances in Pharmacology.

Pomin, V. H., & Mourao, P. A. (2014). Specific sulfation and glycosylation-a structural combination for the anticoagulation of marine carbohydrates. *Frontiers in Cellular and Infection Microbiology, 4*, 33.

Prabhakar, V., & Sasisekharan, R. (2006). The biosynthesis and catabolism of galactosaminoglycans. In N. Volpi (Ed.). *Chondroitin sulfate: Structure, role and pharmacological activity* (pp. 69–115). London: UK Advances in Pharmacology.

Reyers, I., Mussoni, L., Donati, M. B., & de Gaetano, G. (1980). Failure of aspirin at different doses to modify experimental thrombosis in rats. *Thrombosis Research, 18*(5), 669–674.

Rocha, H. A., Moraes, F. A., Trindade, E. S., Franco, C. R., Torquato, R. J., Veiga, S. S., et al. (2005). Structural and hemostatic activities of a sulfated galactofucan from the brown alga Spatoglossum schroederi. An ideal antithrombotic agent? *Journal of*

Biological Chemistry, 280(50), 41278–41288.
Sassaki, G. L., Elli, S., Rudd, T. R., Macchi, E., Yates, E. A., Naggi, A., et al. (2013). Human (α-2,6) and avian (α-2,3) sialylated receptors of influenza A virus show distinct conformations and dynamics in solution. *Biochemistry, 52*(41), 7217–7230.
Schiller, J., Becher, J., Möller, S., Lemmnitzer, K., Riemer, T., & Schnabelrauch, M. (2015). Characterization and chemical modification of glycosaminoglycans of the extracellular matrix. In M. Gama, & H. B. Nader (Eds.). *Sulfated polysaccharides* (pp. 73–104). New York: Nova Science Pub Inc.
Sugahara, K., Mikami, T., Uyama, T., Mizuguchi, S., Nomura, K., & Kitagawa, H. (2003). Recent advances in the structural biology of chondroitin sulfate and dermatan sulfate. *Current Opinion in Structural Biology, 13*(5), 612–620.
Sugahara, K., Tanaka, Y., Yamada, S., Seno, N., Kitagawa, H., Haslam, S. M., et al. (1996). Novel sulfated oligosaccharides containing 3-O-sulfated glucuronic acid from king crab cartilage chondroitin sulfate K. Unexpected degradation by chondroitinase ABC. *Journal of Biological Chemistry, 271*(43), 26745–26754.
Tomatsu, S., Shimada, T., Patel, P., Mason, R. W., Mikami, T., Kitagawa, H., et al. (2015). Chondroitin and keratan sulfate. In M. Gama, H. B. Nader, & H. A. O. Rocha (Eds.). *Sulfated polysaccharides* (pp. 17–71). New York: Nova Science Pub Inc.
Trindade, E. S., Oliver, C., Jamur, M. C., Rocha, H. A., Franco, C. R., Boucas, R. I., et al. (2008). The binding of heparin to the extracellular matrix of endothelial cells up-regulates the synthesis of an antithrombotic heparan sulfate proteoglycan. *Journal of Cellular Physiology, 217*(2), 328–337.
Uniewicz, K. A., Ori, A., Xu, R., Ahmed, Y., Wilkinson, M. C., Fernig, D. G., et al. (2010). Differential scanning fluorimetry measurement of protein stability changes upon binding to glycosaminoglycans: A screening test for binding specificity. *Analytical Chemistry, 82*(9), 3796–3802.
Vilela-Silva, A. C., Werneck, C. C., Valente, A. P., Vacquier, V. D., & Mourao, P. A. (2001). Embryos of the sea urchin strongylocentrotus purpuratus synthesize a dermatan sulfate enriched in 4-O- and 6-O-disulfated galactosamine units. *Glycobiology, 11*(6), 433–440.
Volpi, N. (2011). Anti-inflammatory activity of chondroitin sulphate: New functions from an old natural macromolecule. *Inflammopharmacology, 19*(6), 299–306.
Voshol, H., van Zuylen, C. W., Orberger, G., Vliegenthart, J. F., & Schachner, M. (1996). Structure of the HNK-1 carbohydrate epitope on bovine peripheral myelin glycoprotein P0. *Journal of Biological Chemistry, 271*(38), 22957–22960.
Wang, S., Sugahara, K., & Li, F. (2016). Chondroitin sulfate/dermatan sulfate sulfatases from mammals and bacteria. *Glycoconjugate Journal, 33*(6), 841–851.
Wu, M., Wen, D., Gao, N., Xiao, C., Yang, L., Xu, L., et al. (2015). Anticoagulant and antithrombotic evaluation of native fucosylated chondroitin sulfates and their derivatives as selective inhibitors of intrinsic factor Xase. *European Journal of Medicinal Chemistry, 92*, 257–269.
Yamada, S., & Sugahara, K. (2008). Potential therapeutic application of chondroitin sulfate/dermatan sulfate. *Current Drug Discovery Technologies Journal, 5*(4), 289–301.
Yamagata, T., Saito, H., Habuchi, O., & Suzuki, S. (1968). Purification and properties of bacterial chondroitinases and chondrosulfatases. *Journal of Biological Chemistry, 243*(7), 1523–1535.
Zhang, Z., Weiwer, M., Li, B., Kemp, M. M., Daman, T. H., & Linhardt, R. J. (2008). Oversulfated chondroitin sulfate: Impact of a heparin impurity, associated with adverse clinical events, on low-molecular-weight heparin preparation. *Journal of Medicinal Chemistry, 51*(18), 5498–5501.